Stem Cell Rev and Rep (2017) 13:287–298
DOI 10.1007/s12015-016-9705-1

Endogenous Stem Cells Were Recruited by Defocused Low-Energy Shock Wave in Treating Diabetic Bladder Dysfunction

Yang Jin[1] · Lina Xu[2] · Yong Zhao[2] · Muwen Wang[2] · Xunbo Jin[2] · Haiyang Zhang[2,3]

Published online: 5 December 2016

Abstract Defocused low-energy shock wave (DLSW) has been shown effects on activating mesenchymal stromal cells (MSCs) in vitro. In this study, recruitment of endogenous stem cells was firstly examined as an important pathway during the healing process of diabetic bladder dysfunction (DBD) treated by DLSW in vivo. Neonatal rats received intraperitoneal injection of 5-ethynyl-2-deoxyuridine (EdU) and then DBD rat model was created by injecting streptozotocin. Four weeks later, DLSW treatment was performed. Afterward, their tissues were examined by histology. Meanwhile, adipose tissue-derived stem cells (ADSCs) were treated by DLSW in vitro. Results showed DLSW ameliorated voiding function of diabetic rats by recruiting $EdU^{+}Stro\text{-}1^{+}CD34^{-}$ endogenous stem cells to release abundant nerve growth factor (NGF) and vascular endothelial growth factor (VEGF). Some EdU^{+} cells overlapped with staining of smooth muscle actin. After DLSW treatment, ADSCs showed higher migration ability, higher expression level of stromal cell-derived factor-1 and secreted more NGF and VEGF. In conclusion, DLSW could ameliorate DBD by recruiting endogenous stem cells. Beneficial effects were mediated by secreting NGF and VEGF, resulting into improved innervation and vascularization in bladder.

✉ Haiyang Zhang
zhyhope77@163.com

[1] Hepatobiliary and Enteric Surgery Center, Xiangya Hospital, Central South University, Changsha 410008, China

[2] Minimally Invasive Urology Center, Shandong Provincial Hospital affiliated to Shandong University, 324 Jing5 Wei7 Road, Jinan 250021, China

[3] Knuppe Molecular Urology Laboratory, Department of Urology, School of Medicine, University of California, San Francisco, CA 94143, USA

Keywords adipose tissue-derived stem cells · angiogenesis · defocused low-energy shock wave · mesenchymal stromal cells · vascular endothelial growth factor

Introduction

In recent years, defocused low-energy shock wave (DLSW) therapy has been considered as an effective treatment modality in regeneration medicine, as seen in newly published studies [1–3]. Spectrum of diseases on which DLSW exerted therapeutic effects is increasing, including bone fractures [4], ischemia-induced tissue necrosis [5], peripheral nerve lesions [6], chronic wounds [7], erectile dysfunction [3] and Peyronie's disease [8].

However, the underlying mechanisms of beneficial effect of DLSW are not yet completely understood. Currently, revascularization and inhibition of inflammation induced by shock wave are considered to be the main pathophysiological changes of wound tissues [9, 10]. Expressions of various proangiogenic factors, such as vascular endothelial growth factor (VEGF) and endothelial nitric oxide synthase (eNOS), could be motivated by DLSW in vivo in diabetic mice, consequently promoting neovascularization [11].

Mesenchymal stromal cells (MSCs), as a great promise in regenerative medicine, were also believed to play important roles in the healing process. Our group firstly reported that secretion and proliferation of bone marrow-derived mesenchymal stromal cells (BMSCs) could be enhanced by DLSW, leading to angiogenesis and nerve regeneration in vitro [12]. This phenomenon was also observed by some other research groups [13, 14]. We further proved multiple signaling pathways of MSCs could be activated by DLSW [15]. In vivo, recruitment of transplanted endothelial progenitor cells towards wound tissues could be promoted by DLSW via upregulating stromal cell-derived factor-1 (SDF-1) [16].

To our knowledge, only two reports including ours found DLSW could recruit endogenous MSCs to the disease sites [3, 17]. However, none of these studies described the fates of recruited stem cells in disease sites, the mechanisms of restoration of damaged tissue, or the pathophysiological improvement triggered by recruited stem cells. To address these issues, in the present study effects of DLSW on endogenous stem cells were examined in a rat model of diabetic bladder dysfunction (DBD), which refers to a range of voiding complaints that are prevalent in clinics with diabetes mellitus (DM).

Material and Methods

Animals

All animal care, treatments, and procedures in this study were approved by Shandong Provincial Hospital. Pregnant Sprague-Dawley rats were purchased from Animal Center of Shandong University. A total of 30 female neonatal pups delivered by these primiparous rats were used for this study. Each pup received intraperitoneal injection of 5-ethynyl-2-deoxyuridine (EdU) (50 mg/kg, C10310, Riobio, Guangzhou, China) immediately after birth, as described previously [18, 19]. At 4 weeks of age, five of these rats were randomly selected to serve as Control group (CON, $n = 5$). The remaining 25 rats were each injected intraperitoneally with 60 mg/kg of streptozotocin (STZ) (18,883–66-4, Sigma-Aldrich, St. Louis, MO, USA), and their blood glucose levels were monitored weekly by checking tail vein blood. Rats with fasting blood glucose of ≥200 mg/dL were designated as diabetic and selected for further tests. A total of 21 such rats were randomized into a diabetic group (DM, $n = 10$) and a diabetic plus DLSW group (DM + SW, $n = 11$).

Shock Wave Treatments

Four weeks after STZ injection, rats in DM + SW group were treated with shock waves. Under anesthesia, each rat was placed in a supine position with lower abdomen shaved. After application of common ultrasound gel on lower abdomen, shock wave treatments were performed by an extracorporeal shock wave machine (derma-PACE device, SANUWAVE, Alpharetta, GA, USA). The shock wave probe was kept in close contact with lower abdomen, and a total of 300 shocks were delivered at energy level of 0.1 mJ/mm^2 and frequency of 120/min. This procedure was repeated 3 times a week for a time course of 4 weeks according to previously published protocol [3].

Conscious Cystometry

Then all rats were subjected to awake cystometry as previously described [20, 21]. Under halothane anesthesia, a polyethylene-90 catheter was implanted into bladder 24 h before conscious cystometry. A second polyethylene-90 tube attached to a latex balloon was placed in the intra-abdominal space to measure abdominal pressure. At the time of cystometry, the bladder was filled via bladder catheter with room-temperature phosphate-buffered saline (PBS) at 0.1 mL/min while recording simultaneous pressure in bladder and abdomen through a pressure transducer with Laboratory View 6.0 software (National Instruments, Austin, TX, USA). Rats were allowed about 20 min for the voiding pattern to stabilize. Thereafter, micturition was recorded for 1 h. Cystometric parameters included: micturition interval, urine volume per void, maximum voiding pressure and residual volume.

Preparation of Tissue Sections

After conscious cystometry, all rats were humanely killed. Their bladders, kidneys, pancreases and bone marrow from femoral cavities were harvested. Bladder samples were divided into 3 parts, 1/3 along with kidneys, pancreases and bone marrow samples were fixed in cold 2% formaldehyde and 0.002% saturated picric acid in 0.1 mol/L. phosphate buffer for 4 h, followed by overnight immersion in buffer containing 30% sucrose. The specimens were then embedded in OCT Compound (Sakura Finetek USA, Torrance, CA, USA) and stored at −80 °C until use. The other 2/3 bladder samples were frozen in liquid nitrogen and then stored at −80 °C until use.

Histological Staining

Frozen tissue samples in OCT Compound were cut at 5 μm, adhered to charged slides, and air dried for 5 min. Then sections were placed in 0.3% H_2O_2/methanol for 10 min, washed twice in PBS for 5 min, and incubated with 3% equine serum in PBS/0.3% Triton X-100 for 30 min at room temperature. Afterward, the tissue section was incubated for 2 h at room temperature with primary antibody, and after PBS rinses, further incubated for 1 h with fluorescein isothiocyanate (FITC) or Texas Red-conjugated anti-mouse or anti-rabbit secondary antibody, followed by staining for 5 min with 40,6-diamidino-2- phenylindole (DAPI, Sigma-Aldrich, St. Louis, MO, USA). Primary antibodies included rabbit anti-Tyrosine hydroxylase (TH) (classical marker of presynaptic sympathetic innervation, AB152, Millipore Corp., Billerica, MA, USA), mouse anti-Smooth muscle actin (SMA) (ab7817, Abcam Inc., Cambridge, MA, USA), rabbit anti-Vesicular acetylcholine transporter (VAChT) (classical marker of presynaptic parasympathetic innervation, ICCB26–1, Accurate Chemicals and Scientific Corp., Westbury, NY, USA), rabbit anti-Collagen IV (ab19808, Abcam Inc., Cambridge, MA, USA), rabbit anti-Stromal cell-derived factor-1 (SDF-1) (sc-28,876, Santa Cruz Biotechnology, Santa Cruz, CA, USA), mouse

anti-Stro-1 (14–6688-80, eBioscience, San Diego, CA, USA) and mouse anti-CD34 (sc-7324, Santa Cruz Biotechnology, Santa Cruz, CA, USA).

For EdU staining, tissue sections were incubated with Cell-Light EdU Apollo567 In Vitro Imaging Kit (C10310, Riobio, Guangzhou, China) for 30 min at room temperature. Bladder sections were also stained according to Masson's trichrome staining protocol (ab150686, Abcam, Cambridge, MA, USA) for smooth muscle histology.

Western Blot Analysis

The frozen bladder samples were lysed on ice in double-distilled water containing 10 mmol/L. Tris (T5912, Sigma-Aldrich, Shanghai, China) and 1 mmol/L. EDTA (798,681, Sigma-Aldrich, Shanghai, China). The homogenate was spun at 12000 rpm for 10 min, and supernatant was recovered as a protein sample, which was measured for protein concentration by means of bicinchoninic acid assay (23,227, Pierce Biotechnology, Rockford, IL, USA). Tissue lysates containing 20 μg of protein were electrophoresed in sodium dodecyl sulfate- polyacrylamide gel (s0179, HaiGene, Haerbin, Heilongjiang, China) electrophoresis and were then transferred onto polyvinylidene difluoride membranes (Bio-Rad Laboratories, Hercules, CA, USA). Detection of protein on the membrane was performed with the ECL kit (RPN2108, Amersham Life Sciences Inc., Arlington Heights, IL, USA) using primary antibodies: rabbit anti-SDF-1 (sc-28,876, Santa Cruz Biotechnology, Santa Cruz, CA, USA), mouse anti-Nerve growth factor (NGF) (sc-365,944, Santa Cruz Biotechnology, Santa Cruz, CA, USA) and rabbit anti-VEGF (sc-13,083, Santa Cruz Biotechnology, Santa Cruz, CA, USA), followed by exposure to X-ray films. All membranes were re-probed with anti-β-actin (66,009–1-Ig, Proteintech Group, Chicago, IL, USA) for internal control. The resulting images were analyzed by Image-Pro Plus 6.0 software (Media Cybernetics, Inc., Rockville, MD, USA) to determine the integrated density value of each protein band. Each sample was examined in triplicate.

Quantification of NGF and VEGF

Frozen bladder samples were immersed in ice-cold Tissue Extraction Reagent (FNN0071, Invitrogen Corp., Camarillo, CA, USA) with protease inhibitors, incubated on ice for 30 min, and centrifugated at 10000 rpm for 5 min. The supernatants were collected and subjected to enzyme-linked immunosorbent assay (ELISA) with NGF commercial kit (FME100107, NovaTeinBio, Cambridge, MA, USA) and VEGF commercial kit (RRV00, R&D Systems China, Shanghai, China). To generate statistically relevant data, each bladder sample was subjected to three independent ELISA experiments.

In Vitro Study

To examine the effects of DLSW on MSCs in vitro, cultured adipose tissue-derived stem cells (ADSCs) were treated by DLSW.

Culture of ADSCs and Shock Wave Treatment

Rat ADSCs at passage 2 (P2) were purchased (RASMD-01001, Cyagen, Suzhou, Jiangsu, China), and cultured in commercial medium (RASMD-90011, Cyagen, Suzhou, Jiangsu, China). According to the product description, the ADSCs express positively of CD44, CD90 and CD29, and negatively of CD34, CD11b and CD45. They possess multipotent differentiation abilities into osteocytes, adipocytes and chondrocytes. Cells were passaged when they reached approximately 90% confluence. Shock wave treatment on cultured ADSCs (shocked ADSCs, $n = 3$) was performed by the extracorporeal shock wave machine as previously described protocol [12]. Briefly, the shock wave probe was kept in close contact with the culture flask containing adherent ADSCs by a water-filled cushion covered with common ultrasound gel. The cells were subjected to 800 impulses of DLSW at an energy flux density of 0.1 mJ/mm^2 with a frequency of 120/min. The shock wave treatment was performed before each passage. ADSCs without shock wave treatment (unshocked ADSCs, $n = 3$) were cultured at the same time and served as control.

Cell Morphology Test

The shocked and unshocked ADSCs at passage 4 (P4) above were examined using a microscope with the Axiovision image analysis system (Carl Zeiss, Shanghai, China). To visualize the actin cytoskeleton, ADSCs (P4) were incubated with phalloidin (FITC-conjugated) (P5282, Sigma-Aldrich, St. Louis, MO, USA). Nuclei were counterstained with DAPI. Images were captured by fluorescence microscope (Nikon Ti-S, Nikon Inc., Japan).

ADSCs Labeling with EdU

To assess proliferation, shocked ADSCs (P4) were treated with 10 μmol/L. EdU overnight and were then incubated with Cell-Light EdU Apollo567 In Vitro Imaging Kit at room temperature. Nuclei were counterstained with DAPI. Unshocked ADSCs (P4) were treated in the same way and served as control. Fluorescent images were captured and analyzed with with Image-Pro Plus 6.0 software.

Cell Migration Assay

After shock wave treatment on ADSCs (P4), the culture medium was removed and replaced with 2 mL Dulbecco's

modified Eagle's medium without fetal bovine serum. Twenty-four hours later, the medium was harvested and centrifuged at 1200 rpm for 10 min. The supernatant was recovered and served as conditioned medium (CM). CM of unshocked ADSCs (P4) was collected in the same way. Shocked ADSCs (P4) migratory function was assessed in triplicate using 24-well Biocoat with 8 μm pore size. Briefly, 500 μL shocked ADSCs CM was added to the lower chamber, and 300 μL of medium containing 2×10^5 shocked ADSCs was added to the upper chamber. After incubation for 24 h at 37 °C in a humidified atmosphere with 5% CO_2, migrated cells, which adhered to the lower surface of a glass cover slide, were stained with calcein (C3100, Corp., Camarillo, CA, USA) for 10 min and counted in high-power microscopic fields. Unshocked ADSCs (P4) were treated with unshocked ADSCs CM in the same way and served as control.

SDF-1 Expression Examination

The shocked ADSCs (P4) and unshocked ADSCs (P4) were lysed in a lysis buffer (Beyotime Biotechnology, Haimen, Jiangsu, China) with 1% phenylmethanesulfonyl fluoride and 1% phosphatase inhibitor for 30 min. The homogenate was centrifuged at 12000 rpm for 30 min, and the supernatant was recovered as a protein sample. Then SDF-1 expressions were examined by western blot with the protocol described above.

Quantification of NGF and VEGF

CM of shocked ADSCs (P4) and unshocked ADSCs (P4) were prepared and subjected to ELISA using the protocols described above with NGF commercial kit (FME100107, NovaTeinBio, Cambridge, MA, USA) and VEGF commercial kit (RRV00, R&D Systems China, Shanghai, China).

Image and Statistical Analysis

Images were captured by fluorescence microscope (Nikon Ti-S, Nikon Inc., Japan), and digital histomorphometric analysis was performed with Image-Pro Plus 6.0 software. To determine expressions of TH, VAChT, Collagen IV, and smooth muscle content in bladder samples, the images were scanned with Aperio ImageScope program (Aperio Technologies, Inc., Vista, CA, USA) and analyzed with Aperio positive pixel count algorithm (Aperio Technologies, Inc., Vista, CA, USA) similar to methods previously described [22]. The examination with each sample was performed in triplicate with three high power fields counted at ×400 magnification at each section. The positivity (number of positive pixels over total number of pixels) of each slide was obtained for statistical analysis. For tracking EdU^+ cells in kidney, pancreas, bone marrow and bladder, ratios of EdU^+ cells versus all cells were determined per field by Image-Pro Plus 6.0 software. Each sample was performed in triplicate with five fields. To determine expression of SDF-1 in bladder tissue, SDF-1-positve cells were counted at ×400 magnification. For study in vitro, EdU^+ ADSCs were shown as ratio of labeled nuclei versus total nuclei. For each section, three high-power fields were detected and each measurement was performed in triplicate.

Data were analyzed with the use of Prism 5 (GraphPad Software, San Diego, CA, USA) and expressed as mean ± standard error for continuous variables. Continuous data were compared among groups by using one-way analysis of variance. Tukey-Kramer test was used for post-hoc comparisons. To evaluate bladder functions examined by conscious cystometry among groups, Chi-Square test was performed with Fisher's Exact Test. Statistical significance was set at $p < 0.05$.

Results

DLSW Restored Damaged Bladder Function Induced by Diabetes Mellitus

Representative cystometric graphs of rats displaying normal and abnormal voiding patterns are shown in Fig. 1a. All rats in CON group manifested a normal voiding pattern (Fig. 1b), with a voiding frequency of 8 to 9 times per 30 min during cystometry. During each voiding episode, the net bladder pressure gradually increased with a maximum voiding pressure at 37.2 ± 8.8 cmH_2O before urination, with 0.3 ± 0.1 mL urine volume per void. All rats in the DM group manifested an abnormal pattern (Fig. 1b), with a voiding frequency of 1 to 2 times per 30 min. Bladder was unstable before urination showing many small pressure waves. The maximum voiding pressure was 52.3 ± 11.3 cmH_2O, with a discrete voided amount of 2.5 ± 1.6 mL. A significant proportion of rats in DM + SW (63.6%, $p < 0.01$ versus DM group) had normal voiding pattern (Fig. 1b), with maximum voiding pressure at 45.9 ± 13.8 cmH_2O and 1.5 ± 0.5 mL urine per void. Cystometric pamameters are summarized in Table 1. The significant shorter micturition interval ($p < 0.001$), smaller urine volume per void ($p < 0.05$) and lower maximum voiding pressure ($p < 0.05$) in DM + SW group relative to DM group suggest that contractile function of bladder is preserved after shock wave treatment.

DLSW Enhanced Regenerations of Innervation, Vascularization and Muscle Content of Bladder

To assess pathophysiological changes of diabetic bladder triggered by DLSW, immuno- fluorescence staining of TH and VAChT for evaluating innervation, Collagen IV for evaluating vascularization and Masson's trichrome staining for evaluating muscle content were performed (Fig. 2a). TH, as a classical marker of presynaptic sympathetic innervation, and VAChT, as a classical marker of presynaptic parasympathetic

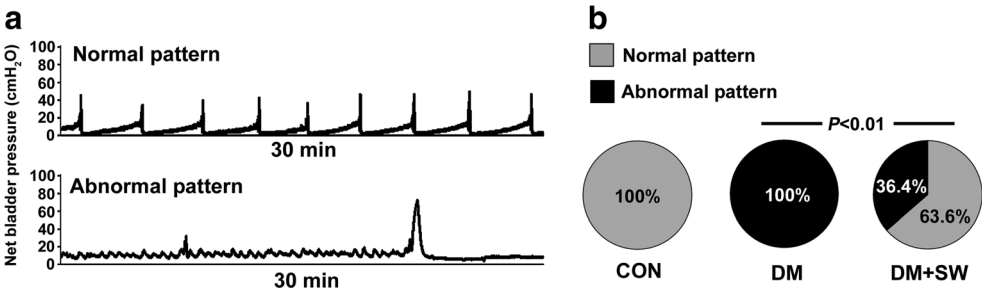

Fig. 1 Assessment of voiding function with conscious cystometry. **a** Representative normal and abnormal voiding patterns (CON, $n = 5$; DM, $n = 10$; DM + SW, $n = 11$). **b** Normal voiding pattern was significantly more common ($p < 0.01$) in DM + SW group compared with DM group

innervation, were most prevalent in smooth muscle regions. Results of counting positive pixels showed significant increase in TH ($p < 0.05$) and decrease in VAChT ($p < 0.01$) in DM group versus CON group. The TH ($p < 0.05$) staining and VAChT ($p < 0.05$) staining were significantly improved in DM + SW group versus DM group (Fig. 2b). A dense and continuous network of collagen IV-positive capillaries was detected below the urothelium in CON group (Fig. 2a). In DM group, collagen IV-positive capillaries network lost continuity or deficient in some areas (DM versus CON: $p < 0.01$). After treatment with DLSW, the damaged collagen IV staining was significantly improved (DM + SW versus DM: $p < 0.05$) (Fig. 2b). Rats in DM group showed a less smooth muscle percent than CON group ($p < 0.05$), which was reversed by DLSW (DM + SW versus DM: $p < 0.05$) (Fig. 2b).

Tracking of EdU$^+$ Cells in Rat Tissues

For investigating the locations of EdU$^+$ cells in rat tissues, the kidney, pancreas, bone marrow and bladder were examined (Fig. 3a). Ratios of EdU$^+$ cells versus all cells were summarized in Fig. 3b. Significantly more EdU$^+$ cells were observed in bladder in DM + SW group ($p < 0.001$, 17.7 ± 7.2%) than DM group(3.7 ± 1.8%). However, the numbers of EdU$^+$ cells in kidney, pancreas, and bone marrow were comparable among groups ($p > 0.05$), respectively.

Expression of SDF-1 and Identification of EdU$^+$ Cells in Bladder

Expressions of SDF-1 in bladder were clearly identified by immunofluorescence staining (Fig. 4a). Meanwhile, some cells co-expressed EdU and SDF-1. SDF-1-positve cells were counted at ×400 magnification, and summarized in Fig. 4b. DM group (4.7 ± 1.6/×400 field) and CON group (3.7 ± 2.2/×400 field) had similar number of SDF-1-positve cells ($p > 0.05$), while DM + SW group (14.6 ± 5.9/×400 field) had significantly more than DM group ($p < 0.001$). Moreover, western blot analysis of bladder tissue (Fig. 4c-d) demonstrated significantly higher ratio of SDF-1/β-actin in DM + SW group than DM group ($p < 0.001$). To identify the EdU$^+$ cells, co-staining of SDF-1 and Stro-1, Stro-1 and EdU, and CD34 and EdU were performed (Fig. 4e-g). Results showed that overlaps between SDF-1 and Stro-1 stains were observed (Fig. 4e). Some EdU$^+$ cells exhibited Stro-1 positivity (Fig. 4f), and EdU$^+$ cells did not express CD34 in the present study (Fig. 4g).

EdU$^+$ Cells Differentiated into Smooth Muscle Cells, and DLSW Enhanced Expressions of NGF and VEGF

Immunofluorescence staining showed that a few EdU$^+$ nuclei appeared to be colocalized with SMA staining in bladder (Fig. 5a). ELISA result (Fig. 5b) of bladder tissue demonstrated that, compared with CON group, NGF ($p < 0.05$) and VEGF ($p < 0.001$) expressed significantly less in DM group, respectively. After treatment of DLSW, NGF ($p < 0.05$) and VEGF ($p < 0.05$) expressed significantly more in DM + SW group than DM group, respectively. In addition, western blot analysis also showed significantly higher ratios of NGF/β-actin ($p < 0.05$) and VEGF/β-actin ($p < 0.01$) in DM + SW group than DM group, respectively (Fig. 5c-d).

Table 1 Comparison of voiding behaviors in conscious cystometry

Cystometric pamameters	Con	DM	DM + SW	*p* value
Micturition interval (s)	234.1 ± 74.6	1528.9 ± 361.2	811.4 ± 423.7*	<0.001
Urine volume per void (mL)	0.3 ± 0.1	2.5 ± 1.6	1.5 ± 0.5**	<0.001
Maximum voiding pressure (cmH_2O)	37.2 ± 8.8	52.3 ± 11.3	45.9 ± 13.8***	<0.05
Residual volume (mL)	0.03 ± 0.01	0.2 ± 0.05	0.2 ± 0.02****	<0.01

Data represented as mean ± standard error, (CON, $n = 5$; DM, $n = 10$; DM + SW, $n = 11$)

$^*p < 0.001$ versus DM, $^{**}p < 0.05$ versus DM, $^{***}p < 0.05$ versus DM, $^{****}p > 0.05$ versus DM

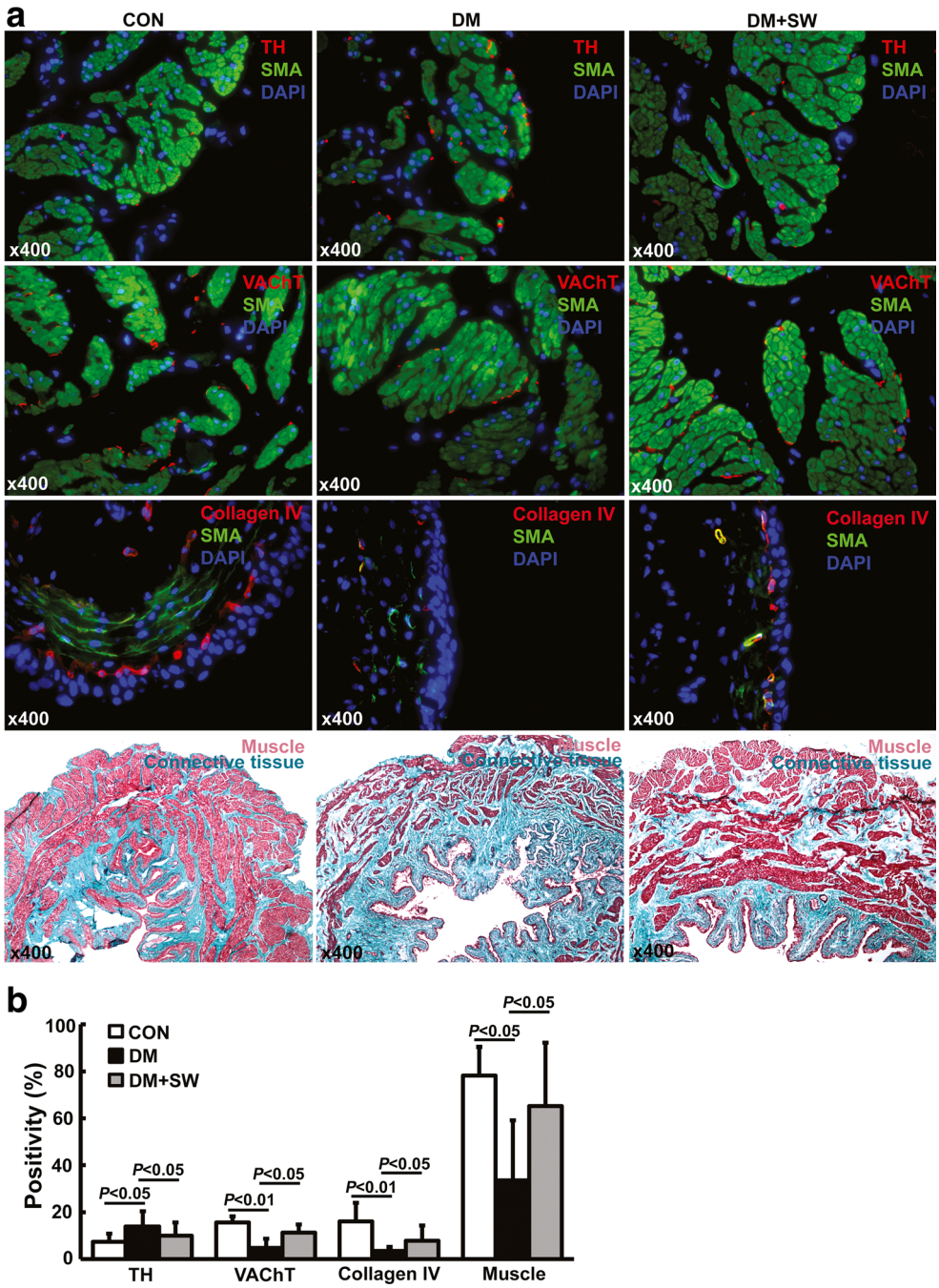

Fig. 2 Representative photomicrographs showing pathophysiological changes of bladder induced by DLSW. **a** Expressions of TH, VAChT and collagen IV were assessed by immunofluorescence staining. TH and VAChT were most prevalent in smooth muscle regions (upper two panels). Collagen IV staining showed a suburothelial capillary network (the third panel). This network was densely stained and continuous in CON group, and was fragmented in DM group. The network integrity was greater in DM + SW group relative to DM group. Masson's trichrome stain showed bladder wall smooth muscle content (*red areas*) was greater in DM + SW group than in DM group (bottom panel). The examination with each sample was performed in triplicate with three high power fields counted at ×400 magnification at each section (CON, $n = 5$; DM, $n = 10$; DM + SW, $n = 11$). **b** The ratios of positivity of TH, VAChT, collagen IV and smooth muscle were presented in the bar chart. Positivity (%) was used to describe the number of positive pixels over the total number of pixels of each sample

ADSCs Were Activated by DLSW in Vitro

ADSCs (P4) showed elongated, spindle-shaped cell bodies. Shock wave treatment did not obviously change their morphological appearances. F-actin cytoskeleton was stained fluorescently by phalloidin, showing a slightly increased alignment of fibers after DLSW treatment without significant differences between two groups (Fig. 6a).

To assess proliferation, EdU labeling and staining of ADSCs were performed. EdU was incorporated into the nuclei of ADSCs (P4) (Fig. 6b). Shocked ADSCs (63.8 ± 9.5%) showed a significantly higher ($p < 0.05$) ratio of EdU^+ cells compared with unshocked ADSCs (35.6 ± 17.7%) (Fig. 6c).

In the cell migration assay, there were significantly more migrated cells ($p < 0.01$) using shocked ADSCs CM (26.4 ± 8.8) than unshocked ADSCs CM (10.1 ± 3.5) (Fig. 6d-e).

Western blot analysis (Fig. 6f-g) demonstrated significantly higher ratio of SDF-1/β-actin in shocked ADSCs than unshocked ADSCs ($p < 0.05$).

ELISA results showed that, compared with unshocked ADSCs CM, shocked ADSCs CM contained significantly

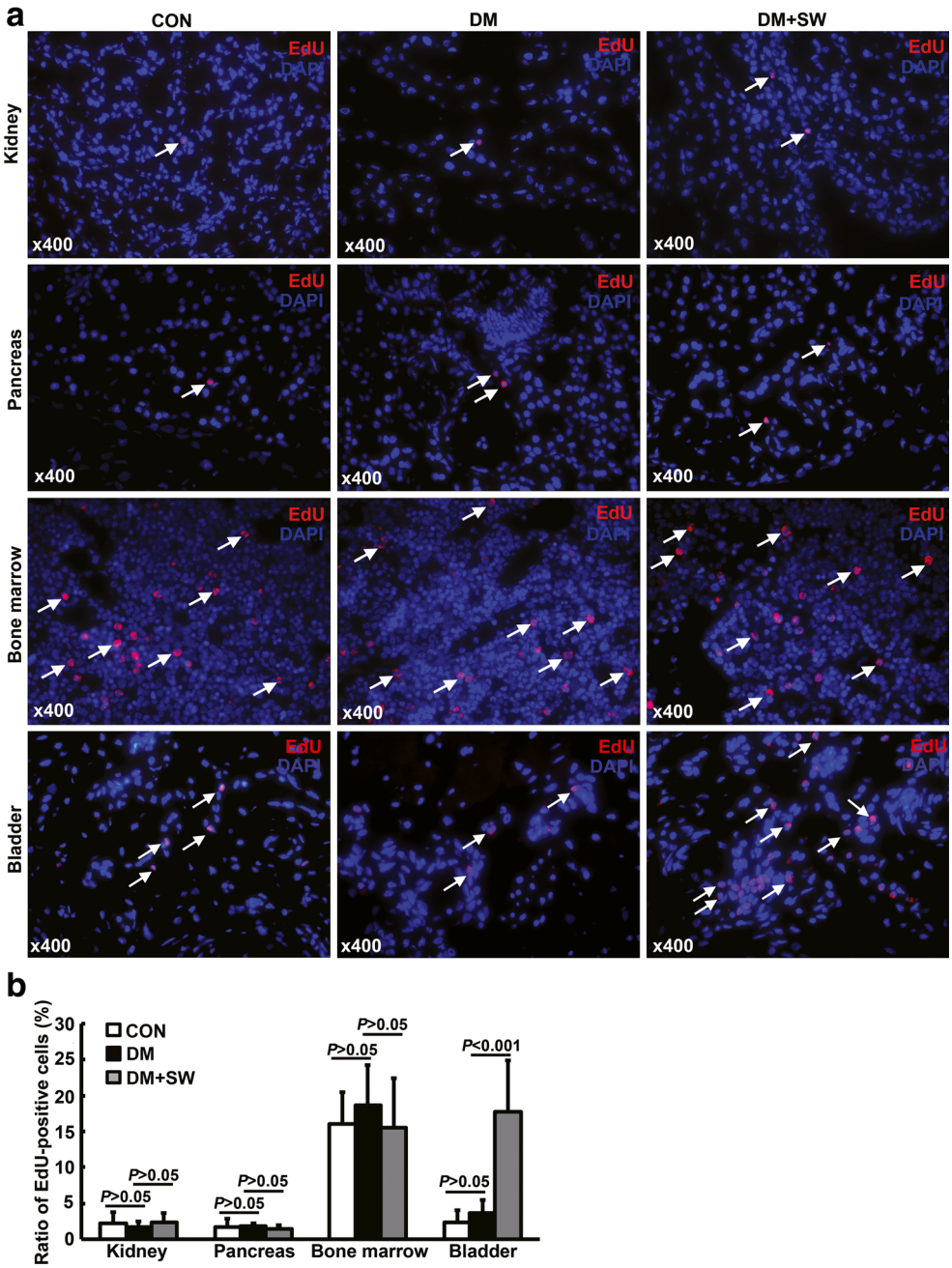

Fig. 3 Tracking of EdU$^+$ cells in rat tissues. **a** Tracking of EdU$^+$ cells in kidney, pancreas, bone marrow and bladder tissues of rats. Each sample was performed in triplicate with five fields (CON, $n = 5$; DM, $n = 10$; DM + SW, $n = 11$). **b** The ratios of EdU$^+$ cells versus all cells were counted by Image-Pro Plus 6.0 software

higher levels of NGF ($p < 0.05$) and VEGF ($p < 0.05$) (Fig. 6h).

Discussion

DBD typically demonstrates in a time-dependent progression of both storage and voiding problems, including urinary frequency, urgency and atonic bladder. The protean feature of DBD is due in large part to a variety of physiological insults induced by hyperglycemia, including damaged smooth muscle cells (SMCs), neuropathy, and urothelial dysfunction [23]. DBD patients are often refractory to traditional managements which are designed to mitigate symptoms rather than treat the underlying disorders. In the past decade, several novel paradigms for treating DBD have been explored. In 2012, we applied ADSCs for the first time to treat DBD [20]. Results showed ADSCs transplantation ameliorated voiding dysfunction by paracrine pathway, and partly by differentiation into SMCs. In the present study, DLSW was firstly introduced to treat DBD. Based on cystometric analysis, all rats in DM group had voiding dysfunction, whereas only 36.4% in DM + SW group had voiding dysfunction 1 month after applying DLSW. This satisfactory result was beyond our

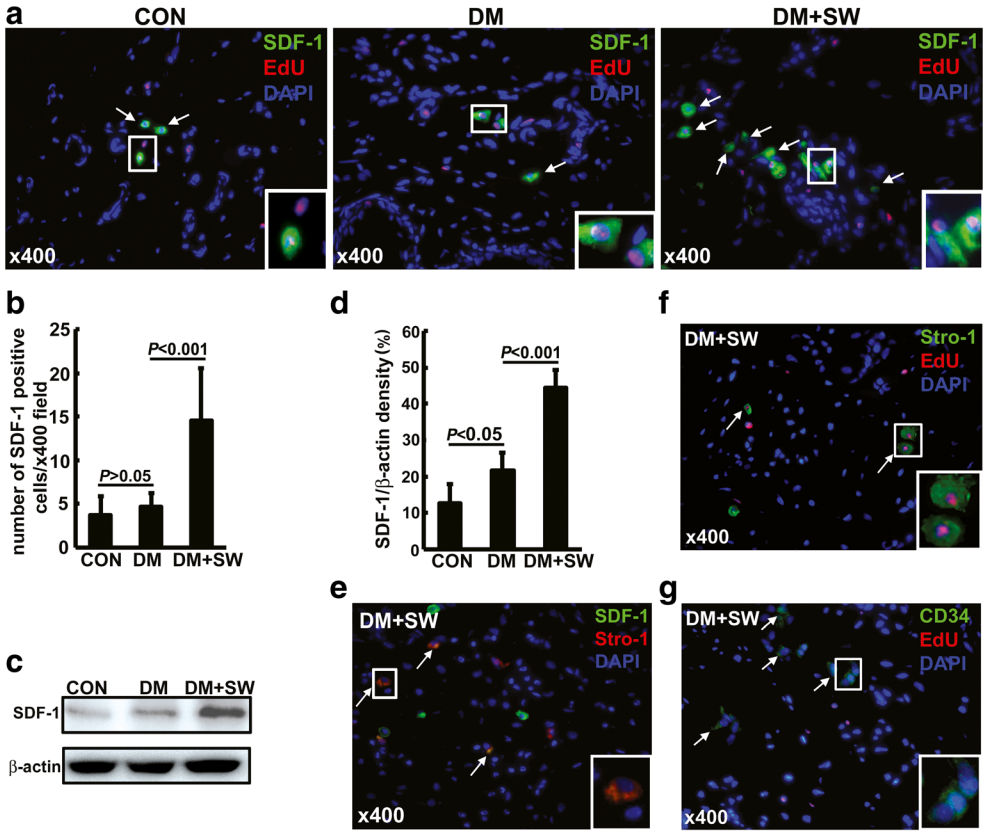

Fig. 4 Identification of EdU$^+$ cells in bladder (CON, $n = 5$; DM, $n = 10$; DM + SW, $n = 11$). **a** Bladder tissues from 3 groups were stained with SDF-1 antibody. Expressions of SDF-1 (*white arrows*) were clearly detected in bladder tissue sections. Some cells (boxed areas) co-expressed EdU and SDF-1. **b** Numbers of SDF-1-positve cells at ×400 magnification were counted by Image-Pro Plus 6.0 software. **c** Western blot analysis of expressions of SDF-1 in bladder tissues. β-actin served as control. **d** Ratios (in percentile) of SDF-1/β-actin were determined by dividing the densitometric values of these protein bands obtained from western blot. **e** Immunofluorescence staining showed some SDF-1$^+$ cells were colocalized with Stro-1 staining (white arrows). **f** A few EdU$^+$ nuclei were colocalized with Stro-1 staining (*white arrows*). **g** CD34$^+$ cells were detected by immunofluorescence staining (*white arrows*). However, EdU$^+$ cells were CD34$^-$ cells. Boxed areas are enlarged into lower-right-corner boxes (×1000 magnification), respectively

expectations because these rats continue to be hyperglycemic after DLSW treatment. We are wondering whether a better outcome could be achieved by increasing DLSW treatment times, or by extending treatment duration along with correction of hyperglycemia. DLSW is likely to be an effective therapeutic option with great advantages in the future because of its facilitation and non-invasiveness.

DLSW has been considered as an effective therapeutic strategy in regenerative medicine for several decades. Besides some routine mechanisms, such as revascularization and antibacterial action, activation of MSCs were believed to play an important role in the healing process of DLSW [3, 9, 12, 13]. Up to date, several research groups have dedicated themselves to this promising field. In 2013, our study in vitro firstly reported that activation of BMSCs might be a new mechanism of DLSW in regenerative medicine by enhancing the secretion and proliferation of BMSCs, and subsequent angiogenesis and nerve repair [12]. Our results in the present study showed DLSW could not interfere the morphology and f-actin cytoskeleton of ADSCs, which is consistent with previous researches [13, 15]. In addition, many studies have reported that DLSW did not change the phenotype or differentiation of cultured MSCs [12, 13, 15]. However, evidences that DLSW could also exert its influence on endogenous stem cells in vivo are still lacking nowadays. Thus, the present study was designed to assess, for the first time, the effects of DLSW on endogenous stem cells and identify the recruited endogenous stem cells tentatively by using a well-established DBD rat model.

EdU, a new thymidine analog, could be incorporated into the nuclear DNA and, therefore, makes it easier to colocalize with DAPI [18]. EdU staining procedure does not require treating the tissue sample with any harsh chemicals, thus allowing detection of cellular differentiation [24]. EdU label-retaining method has been a frequently employed approach for identification of resident or migrated stem cells in postnatal tissues [3, 20, 25]. In the present study, this strategy was repeated for identifying the migrated stem cells in various organs of rats. The results showed that diabetic rats with DLSW had significantly more EdU$^+$ cells in bladder than diabetic rats

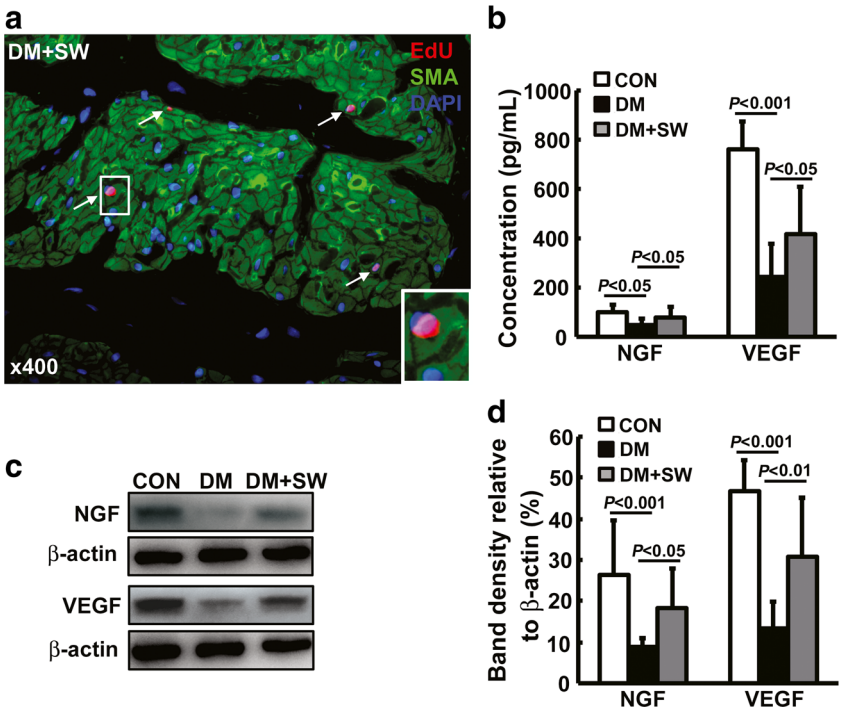

Fig. 5 EdU$^+$ cells' differentiation ability and quantification of NGF and VEGF in bladder. **a** Immunofluorescence staining showed some EdU$^+$ cells were colocalized with SMA (*white arrows*). Boxed area is enlarged into lower-right-corner box (×1000 magnification). **b** Expressions of NGF and VEGF in bladder tissues of 3 groups were compared by ELISA. **c** Western blot analysis of expressions of NGF and VEGF in bladder tissues. β-actin served as control. **d** Ratios (in percentile) of NGF/β-actin and VEGF/β-actin were determined by dividing the densitometric values of these protein bands obtained from western blot

without DLSW, suggesting an increased recruitment of endogenous stem cells. Moreover, in vitro study, shocked ADSCs expressed more EdU suggested that ADSCs acquired stronger proliferation ability after DLSW treatment.

Actually as early as 2004, recruitment of endogenous MSCs were reported in the early stage of shock wave-promoted bone regeneration of segmental defect in rats [17]. RP59, a not commonly used marker of MSCs that was also detected in erythroid cells and megakaryocytes [26], was applied to label the recruited MSCs which were indicated as MSCs by the authors. The accuracy of identification of MSCs just by RP59-positivity and "round- and cuboidal-shaped cells" is questionable. In 2013, in a rat model of erectile dysfunction, we found beneficial effect of DLSW was mediated by recruitment of endogenous stem cells through EdU label-retaining strategy [3]. However, in that study we did not provide convincing evidences to prove MSCs' identities and their differentiation capacities as narrated in discussion. CD73, CD90 and CD105, the commonly used MSCs markers, are co-expressed in a wide variety of cells, and no verifiable evidences support that they are certainly capable of identifying MSCs in vivo, even when used in combination [24]. Therefore, in the present study, Stro-1, by far the best-known MSCs marker despite its concurrent expression in endothelium [24, 27], was selected as the MSCs' identifying marker. CD34, another controversial stem cell marker, is generally considered as a negative MSCs marker except some specific MSCs sources, such as adipose tissue-derived MSCs [24]. In the present study, some EdU$^+$ cells recruited into bladder were proved to be Stro-1$^+$ and CD34$^-$ cells. However, because of the existence of EdU$^+$Stro-1$^-$ cells and lack of specific markers, more evidences should be provided in the future to identify the EdU$^+$ cells. Moreover, SDF-1, an important chemotactic factor of MSCs, was co-expressed in some EdU$^+$ and Stro-1$^+$ cells in an increasing trend with DLSW, suggesting the migration of stem cells triggered by DLSW might be mediated by increasing SDF-1 in disease site. This phenomenon was further supported by the results in vitro that ADSCs expressed more SDF-1 after shock wave treatment.

Regarding to by which way the recruited endogenous stem cells exerted their functions, the results showed some of the EdU$^+$ nuclei appeared to reside within cells expressing SMA, thus suggesting that a small fraction of recruited endogenous stem cells may have differentiated into SMCs. The relative paucity of EdU$^+$ cells in bladder implies that the differentiation pathway plays at a minor role in therapeutic effects of DLSW. In addition, it is difficult to interpret the improvements of innervation and vascularization in bladder by endogenous stem cells' differentiation ability on account of lacking EdU$^+$ cells concurrently expressed neural or vascular markers. Hence, it is logical to deduce that paracrine functions of recruited endogenous stem cells or their neighboring cells by releasing a variety of cytokines and growth factors are responsible for the therapeutic effects. We have proved in vitro that DLSW enhanced regenerations of nerve and blood vessel via upregulating MSCs' secretions of VEGF, NGF and CXC ligand 5 (CXCL5) [12, 15]. In the present study, this result was repeated on cultured ADSCs. The restorations of neural markers, TH and VAChT, and vascular marker, collagen IV, could also be interpreted by this mechanism.

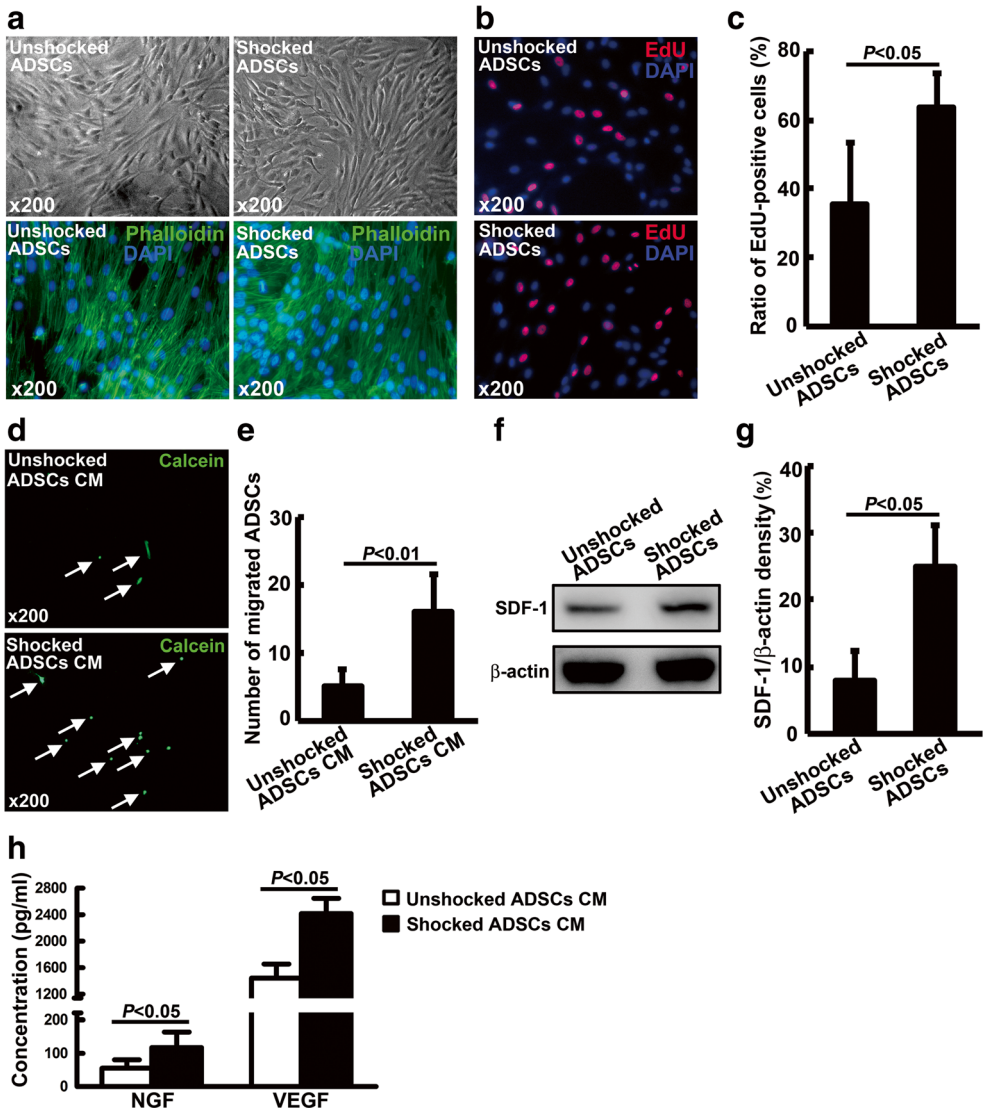

Fig. 6 DLSW activated ADSCs in vitro (unshocked ADSCs, $n = 3$; shocked ADSCs, $n = 3$). **a** The morphology of cultured ADSCs (P4) was observed using a microscope (*upper panel*). F-actin cytoskeleton was stained with phalloidin (*lower panel*). **b** To assess the effect of shock waves on proliferation, unshocked and shocked ADSCs (P4) were labeled with 10 μmol/L. EdU and counterstained with DAPI. **c** Digital histomorphometric analysis of ratio of EdU^+ ADSCs (the ratio between EdU-labeled cells and DAPI-labeled cells) per field was performed with Image-Pro Plus 6.0 software. **d** The migration ability in vitro was examined using cell migration assay (The migrated cells were indicated with white arrows). **e** The migrated ADSCs were counted in high-power microscopic field. **f** Western blot analysis of expressions of SDF-1 in cultured ADSCs. β-actin served as control. **g** Ratios (in percentile) of SDF-1/β-actin were determined by dividing the densitometric values of these protein bands obtained from western blot. **h** Concentrations of NGF and VEGF in CM of shocked and unshocked ADSCs were compared using ELISA

Several considerations should be noted before conclusion. 1) Upon all the observations in the present and previous studies, a hypothesis of the role of stem cells in healing process of DLSW in regeneration medicine could be put forward (Fig. 7). The first event in the process is that the stem cells in the local site/disease site receive stimulations from DLSW. Then, the local stem cells will be activated via phosphorylations of internal mitogen-activated protein kinases (MAPK) pathway,

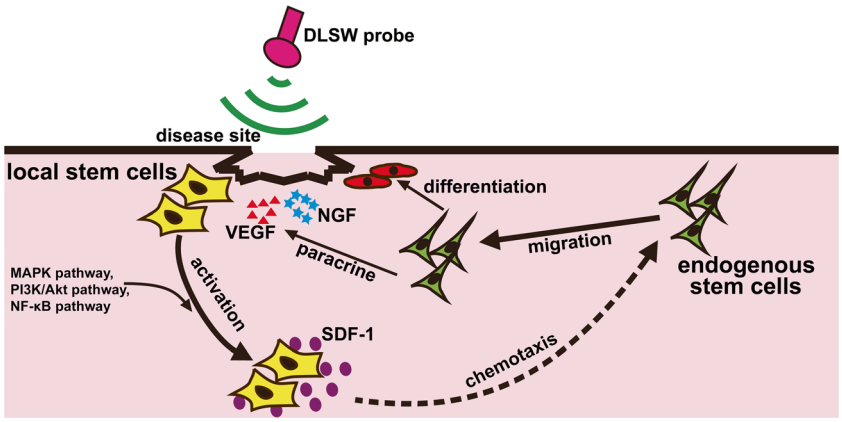

Fig. 7 Hypothesis of mechanism of the roles of stem cells in healing process of DLSW in regenerative medicine

phosphoinositide 3-kinase (PI3K)/Akt pathway and nuclear factor-kappa B (NF-κB) signaling pathway [15], resulting into expressing more chemotactic factors, such as SDF-1. Then numerous endogenous stem cells in distance will migrate to the disease site and acquire activation from DLSW stimulation. They exert their therapeutic effects not only through differentiating into the defect tissue types, but also through secreting a large scale of nutrition factors, growth factors and anti-inflammation factors as a major role, such as VEGF, NGF and CXCL5, leading to improving innervation and vascularization in the disease site. 2) In the present study, several types of cells with different staining outcomes were not identified, including $EdU^{+}Stro\text{-}1^{-}$ cells, $EdU^{-}SDF\text{-}1^{+}$ cells and $CD34^{+}$ cells. This problem need to be investigated. 3) Though DLSW could stimulate stem cells to secrete more cytokines and growth factors in vitro [12, 15], evidences in vivo supporting that the increased NGF and VEGF were released by stem cells, not by neighboring cells, are still lacking.

Conclusion

The findings provided by the present study suggest that activation of endogenous stem cells plays a key role in the regenerative process triggered by DLSW. These beneficial effects appear to be mediated by secreting more NGF and VEGF from recruited endogenous stem cells, resulting into improved innervation and vascularization in bladder.

Acknowledgements The authors thank Qinghua Xia and Shaobo Jiang, Minimally Invasive Urology Center, Shandong Provincial Hospital affiliated to Shandong University, Jinan, China, for their assistance throughout this study.

Compliance with Ethical Standards

Funding This work was supported by the National Natural Science Foundation of China (81300629).

Conflict of Interest The authors declare that they have no conflict of interest.

References

1. Kisch, T., Wuerfel, W., Forstmeier, V., Liodaki, E., Stang, F. H., Knobloch, K., et al. (2016). Repetitive shock wave therapy improves muscular microcirculation. *Journal of Surgical Research, 201*, 440–445.
2. Sheu, J. J., Lee, F. Y., Yuen, C. M., Chen, Y. L., Huang, T. H., Chua, S., et al. (2015). Combined therapy with shock wave and autologous bone marrow-derived mesenchymal stem cells alleviates left ventricular dysfunction and remodeling through inhibiting inflammatory stimuli, oxidative stress & enhancing angiogenesis in a swine myocardial infarction model. *International Journal of Cardiology, 193*, 69–83.
3. Qiu, X., Lin, G., Xin, Z., Ferretti, L., Zhang, H., Lue, T. F., et al. (2013). Effects of low-energy shockwave therapy on the erectile function and tissue of a diabetic rat model. *The Journal of Sexual Medicine, 10*, 738–746.
4. Furia, J. P., Juliano, P. J., Wade, A. M., Schaden, W., & Mittermayr, R. (2010). Shock wave therapy compared with intramedullary screw fixation for nonunion of proximal fifth metatarsal metaphyseal-diaphyseal fractures. *Journal of Bone and Joint Surgery (American), 92*, 846–854.
5. Mittermayr, R., Hartinger, J., Antonic, V., Meinl, A., Pfeifer, S., Stojadinovic, A., et al. (2011). Extracorporeal shock wave therapy (ESWT) minimizes ischemic tissue necrosis irrespective of application time and promotes tissue revascularization by stimulating angiogenesis. *Annals of Surgery, 253*, 1024–1032.
6. Hausner, T., Pajer, K., Halat, G., Hopf, R., Schmidhammer, R., Redl, H., et al. (2012). Improved rate of peripheral nerve regeneration induced by extracorporeal shock wave treatment in the rat. *Experimental Neurology, 236*, 363–370.
7. Mittermayr, R., Antonic, V., Hartinger, J., Kaufmann, H., Redl, H., Teot, L., et al. (2012). Extracorporeal shock wave therapy (ESWT) for wound healing: technology, mechanisms, and clinical efficacy. *Wound Repair and Regeneration, 20*, 456–465.
8. Lander, E. B., Berman, M. H., & See, J. R. (2016). Stromal vascular fraction combined with shock wave for the treatment of Peyronie's disease. *Plast Reconstr Surg Glob Open, 4*, e631.
9. Makarevich, P. I., Boldyreva, M. A., Gluhanyuk, E. V., Efimenko, A. Y., Dergilev, K. V., Shevchenko, E. K., et al. (2015). Enhanced angiogenesis in ischemic skeletal muscle after transplantation of cell sheets from baculovirus-transduced adipose-derived stromal cells expressing VEGF165. *Stem Cell Research & Therapy, 6*, 204.
10. Kuo, Y. R., Wu, W. S., Hsieh, Y. L., Wang, F. S., Wang, C. T., Chiang, Y. C., et al. (2007). Extracorporeal shock wave enhanced extended skin flap tissue survival via increase of topical blood perfusion and associated with suppression of tissue pro-inflammation. *Journal of Surgical Research, 143*, 385–392.
11. Hayashi, D., Kawakami, K., Ito, K., Ishii, K., Tanno, H., Imai, Y., et al. (2012). Low-energy extracorporeal shock wave therapy enhances skin wound healing in diabetic mice: a critical role of endothelial nitric oxide synthase. *Wound Repair and Regeneration, 20*, 887–895.
12. Zhao, Y., Wang, J., Wang, M., Sun, P., Chen, J., Jin, X., et al. (2013). Activation of bone marrow-derived mesenchymal stromal cells-a new mechanism of defocused low-energy shock wave in regenerative medicine. *Cytotherapy, 15*, 1449–1457.
13. Raabe, O., Shell, K., Goessl, A., Crispens, C., Delhasse, Y., Eva, A., et al. (2013). Effect of extracorporeal shock wave on proliferation and differentiation of equine adipose tissue-derived mesenchymal stem cells in vitro. *Am J Stem Cells, 2*, 62–73.
14. Suhr, F., Delhasse, Y., Bungartz, G., Schmidt, A., Pfannkuche, K., & Bloch, W. (2013). Cell biological effects of mechanical stimulations generated by focused extracorporeal shock wave applications on cultured human bone marrow stromal cells. *Stem Cell Research, 11*, 951–964.
15. Xu, L., Zhao, Y., Wang, M., Song, W., Li, B., Liu, W., et al. (2016). Defocused low-energy shock wave activates adipose tissue-derived stem cells in vitro via multiple signaling pathways. *Cytotherapy, 18*, 1503–1514.
16. Aicher, A., Heeschen, C., Sasaki, K., Urbich, C., Zeiher, A. M., & Dimmeler, S. (2006). Low-energy shock wave for enhancing recruitment of endothelial progenitor cells: a new modality to increase efficacy of cell therapy in chronic hind limb ischemia. *Circulation, 114*, 2823–2830.
17. Chen, Y. J., Wurtz, T., Wang, C. J., Kuo, Y. R., Yang, K. D., Huang, H. C., et al. (2004). Recruitment of mesenchymal stem cells and

expression of TGF-beta 1 and VEGF in the early stage of shock wave-promoted bone regeneration of segmental defect in rats. *Journal of Orthopaedic Research, 22*, 526–534.

18. Lin, G., Huang, Y. C., Shindel, A. W., Banie, L., Wang, G., Lue, T. F., et al. (2009). Labeling and tracking of mesenchymal stromal cells with EdU. *Cytotherapy, 11*, 864–873.
19. Zhang, H., Lin, G., Qiu, X., Ning, H., Banie, L., Lue, T. F., et al. (2012). Label retaining and stem cell marker expression in the developing rat urinary bladder. *Urology, 79*, 746.e741–746.e746.
20. Zhang, H., Qiu, X., Shindel, A. W., Ning, H., Ferretti, L., Jin, X., et al. (2012). Adipose tissue-derived stem cells ameliorate diabetic bladder dysfunction in a type II diabetic rat model. *Stem Cells and Development, 21*, 1391–1400.
21. Huang, Y. C., Shindel, A. W., Ning, H., Lin, G., Harraz, A. M., Wang, G., et al. (2010). Adipose derived stem cells ameliorate hyperlipidemia associated detrusor overactivity in a rat model. *Journal of Urology, 183*, 1232–1240.
22. Lee, M. J., Bagci, P., Kong, J., Vos, M. B., Sharma, P., Kalb, B., et al. (2013). Liver steatosis assessment: correlations among pathology, radiology, clinical data and automated image analysis software. *Pathology, Research and Practice, 209*, 371–379.
23. Yoshimura, N., Chancellor, M. B., Andersson, K. E., & Christ, G. J. (2005). Recent advances in understanding the biology of diabetes-associated bladder complications and novel therapy. *BJU International, 95*, 733–738.
24. Lin, C. S., Xin, Z. C., Dai, J., & Lue, T. F. (2013). Commonly used mesenchymal stem cell markers and tracking labels: limitations and challenges. *Histology and Histopathology, 28*, 1109–1116.
25. Zhang, H., Lin, G., Qiu, X., Ning, H., Banie, L., Lue, T. F., et al. (2012). Label retaining and stem cell marker expression in the developing rat urinary bladder. *Urology, 79*, 746 .e741-746
26. Kruger, A., Ellerstrom, C., Lundmark, C., Christersson, C., & Wurtz, T. (2002). RP59, a marker for osteoblast recruitment, is also detected in primitive mesenchymal cells, erythroid cells, and megakaryocytes. *Developmental Dynamics, 223*, 414–418.
27. Kolf, C. M., Cho, E., & Tuan, R. S. (2007). Mesenchymal stromal cells. Biology of adult mesenchymal stem cells: regulation of niche, self-renewal and differentiation. *Arthritis Research and Therapy, 9*, 204.